Volume Change during the Formation of Nanoporous Gold by Dealloying

S. Parida,[1] D. Kramer,[1] C. A. Volkert,[1] H. Rösner,[1] J. Erlebacher,[2] and J. Weissmüller[1,3,*]

[1]*Forschungszentrum Karlsruhe, Karlsruhe, Germany*
[2]*The Johns Hopkins University, Baltimore, Maryland, USA*
[3]*Universität des Saarlandes, Saarbrücken, Germany*

(Received 24 January 2006; revised manuscript received 16 May 2006; published 20 July 2006)

We report a macroscopic shrinkage by up to 30 vol % during electrochemical dealloying of Ag-Au. Since the original crystal lattice is maintained during the process, we suggest that the formation of nanoporous gold in our experiments is accompanied by the creation of a large number of lattice defects and by local plastic deformation.

DOI: 10.1103/PhysRevLett.97.035504 PACS numbers: 61.72.−y, 61.46.−w

Dealloying is a corrosion process in which the less noble component of a solid solution or compound is selectively removed by chemical or electrochemical means. Besides touching on fundamental issues of alloy thermodynamics and corrosion science [1,2] and providing a means for obtaining high surface area granular metal catalysts such as Raney nickel [3], the process offers the potential to produce monolithic metal bodies with a nanoscale pore structure. Ag-Au alloys form a model system for the latter case, since the continuous solid solubility and the similar atomic volumes of the constituents allow for an essentially coherent transformation from the master alloy to the nanoporous gold (NPG) product structure. The recent interest in NPG is motivated partly by the prospect of applying the material as a heat exchanger [4], a catalyst [5], an actuator [6], or a precursor for producing bulk nanocrystalline gold [7].

The current understanding of the formation of NPG emphasizes atomic rearrangements at the interface between the metal and the solution [8–10]. As silver is dissolved, gold atoms are released from alloy surface terraces and reorganize themselves into clusters. The clusters form the initial surfaces of the ultimately three-dimensionally porous structure, and new gold atoms are supplied to them as dissolution propagates to the next and further atomic layers. Thus, the process is modeled in terms of diffusive redistribution of components (gold and vacancies) on a crystal lattice. Although new ligaments are continuously formed by bifurcation of pores that have sufficiently penetrated into the bulk, the mechanism does not require either nucleation of new crystallites nor the formation or removal of lattice sites.

As the crystal lattice is maintained, one might expect that the overall sample dimensions are invariant during dealloying, so that the pore fraction in NPG reflects the fraction of atoms which are dissolved. However, simultaneous to the formation of porosity, a number of other processes are active, including coarsening behind the dissolution front, various sources of plastic deformation, and capillary forces. Although, in principle, the action of each of these effects is nanoscale in extent, when they are operating uniformly throughout a sample, the results can have startling macroscopic consequences. Here we report the observation of a macroscopic volume reduction by as much as 30% during dealloying. This is not consistent with a process exclusively involving dissolution and diffusion on a rigid lattice.

We studied NPG in two forms: bulk and leaf samples. The master alloy for the bulk samples was prepared by arc melting; the ingots (~4 g) were homogenized by annealing at 850 °C for 100 h in evacuated quartz ampoules, rolled to form sheets 1 mm thick, cut into 1 mm edge-length cubes, and finally annealed for 3 h at 850 °C in Ar flow for recovery. Leaf samples [11] were obtained by dealloying as-received white gold leaf, 120 nm thick, of two qualities: 6 carat (Wasner Blattgold GmbH, Schwabach, Germany) and 11 carat (“Monarch,” Sepp Leaf Products, New York). Energy-dispersive x-ray fluorescence (EDX) data indicate the compositions $Ag_{80}Au_{20}$ and $Ag_{67}Au_{33}$ for the 6 and 11 carat samples, respectively.

Electrochemical dealloying was carried out in perchloric acid (1 M) at ambient temperature under potential control using a potentiostat, Ag/AgCl reference, and Ag counter electrodes. The setup for *in situ* dilatometry was identical to that described previously with relation measurement of the surface stress of porous metals [6,12]. The stress exerted by the dilatometer probe is about 0.02 Pa, insignificantly small in relation to the yield strength of nanoporous gold (~100 MPa) [13]. By optical microscopy, it was verified that the probe does not indent the NPG sample surface and that the NPG samples are free of cracks at the scale of microns or above. Transmission electron microscopy (TEM) studies were done on as-dealloyed leaf samples with a Philips Tecnai F20ST at 200 kV. Focused ion-beam (FIB) microscopy was carried out using a 30 keV Ga ion beam in a Nova NanoLab by the FEI company.

The findings from our TEM investigations, as exemplified by images [Figs. 1(a)–1(e)] of NPG formed at two different dealloying potentials $E_D = 600$ and 850 mV, are as follows: (i) The characteristic ligament size drops with increasing E_D, from 20 to 4 nm in the example. (ii) The

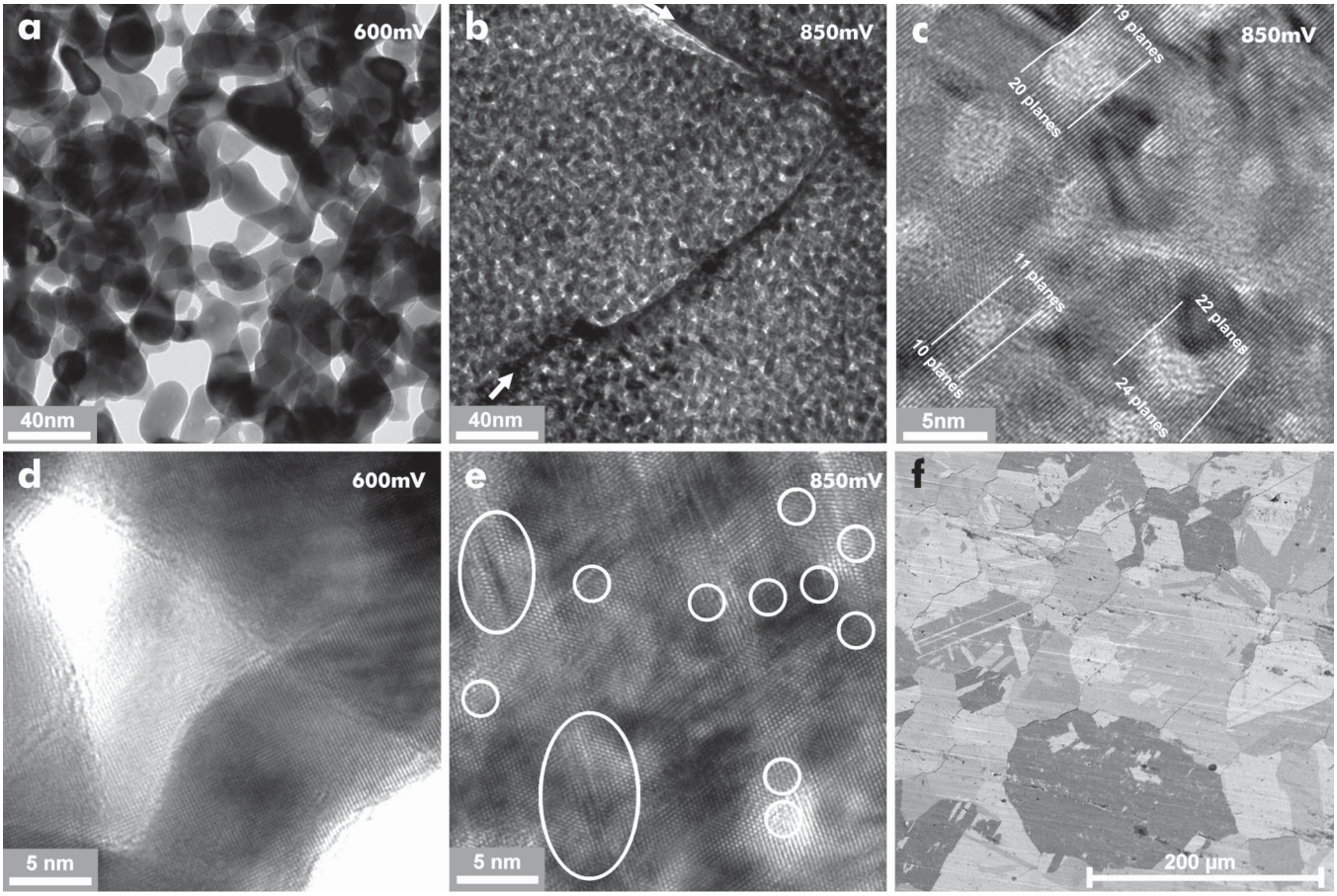

FIG. 1. Micrographs of NPG. (a),(b) Bright-field, (c)–(e) high-resolution transmission electron micrographs of 6 carat gold leaf dealloyed at the potentials indicated. The arrows in (b) mark a high-angle grain boundary. A selection of lattice dislocations and stacking faults are marked by circles and ellipses, respectively, in (e). Some lattice planes end in pores, as indicated in (c). (f) Focused ion-beam image of NPG prepared from bulk $Ag_{75}Au_{25}$.

structure obtained at 600 mV appears much more open. (iii) A very large density of defects (lattice dislocations, stacking faults, and twins) is apparent in the 850 mV material. While the limited statistics of the observations prevents quantifying the defect density, there is a clear trend for more defects at higher E_D. An unusual defect feature is missing lattice planes associated with pores: For the 850 mV material, counting the {111}-lattice fringes on opposite sides of pores reveals a deficit, typically of more than one lattice spacing. (iv) Selected area diffraction, along with the coherent lattice orientation of the high-resolution TEM images, confirms that the entire frame of observation is typically single-crystalline. High-angle grain boundaries, such as that in Fig. 1(b), are extremely rare, consistent with the established notion (see, e.g., Refs. [8,14]) that the crystal lattice orientation is retained during dealloying and with the conservation of the 50–100 μm grain size of the master alloy. This grain structure remains visible in FIB images of NPG [Fig. 1(f)].

By EDX analysis, 4–10 at. % Ag is found in the NPG samples. The deposit at the counter electrode is Ag with ≤ 0.2 at. % Au, showing that Au does not dissolve under the conditions of our experiments.

X-ray diffraction indicates that the lattice parameter is reduced by about 0.3% after dealloying. Remarkably, much larger macroscopic dimension changes were always apparent, as exemplified by the photographs of a leaf sample before and after dealloying (Fig. 2). The vertical and horizontal edge lengths are seen to shorten each by 13% of the original length of 23 mm; in other words, the macroscopic surface area is reduced by 23%.

We have also investigated the dimension change of cubes of bulk $Ag_{75}Au_{25}$ (Fig. 2) during potentiostatic dealloying, using *in situ* dilatometry. Compared to the leaf, the edge length 0.9 mm is here thicker by roughly a factor of 10^4. The results, as exemplified by Figs. 3(a) and 3(b), were consistent with those of the leaf samples. As the sample in Figs. 3(a) and 3(b) is macroscopically isotropic, the net lateral contraction (after complete dealloying) by $\Delta l = 7.3\%$ suggests a net volume reduction by as much as 20%. Figure 3(b) shows that the length varies roughly in proportion to the charge transferred and, therefore, to the amount of Ag removed.

For various E_D, Fig. 3(c) shows the net Δl versus the time $t_{1/2}$ at which half the total dealloying charge was transferred. For leaf as well as bulk samples, shrinkage

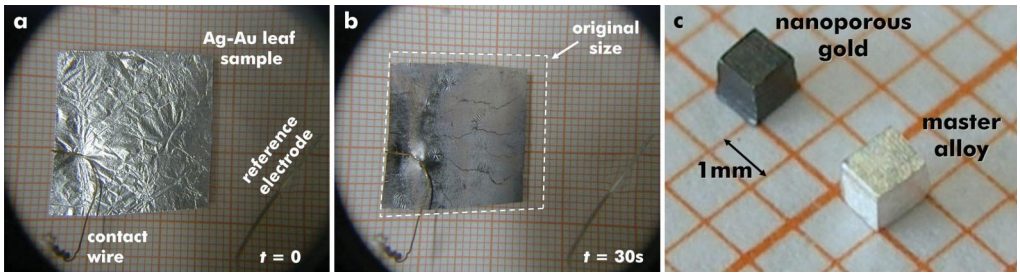

FIG. 2 (color). Photographs of Ag-Au samples. 6 carat leaf sample (a) before and (b) after dealloying, showing an area reduction by about 23%. The leaf is floating on an electrolyte; a ring-shaped counter electrode is located outside the image area. (c) Two bulk samples of about 1 mm^3 volume, master alloy and NPG.

and the dealloying rate are seen to be correlated, with more shrinkage and faster dealloying at higher E_D. This is consistent with the apparent density differences seen in TEM [Figs. 1(a) and 1(b)]. In view of the higher Au fraction in the 11 carat leaf, it is not unexpected that its amount of shrinkage in Fig. 3(c) is less than for the bulk material. Yet, Δl remains significant here.

At first sight, our observation of a reduction in the outer sample dimension may not be surprising in view of the fact that dealloying removes more than half the atoms from the solid solution. Yet, the finding is actually not immediately compatible with models of dealloying, such as that of Refs. [9,10], which work with a rigid lattice: It is compatible with such models to consider a coherent lattice extending throughout both the solid phase and the pore space of NPG, pores being viewed as clusters of lattice sites occupied by vacancies, and we stress that only two elementary steps are considered, (i) dissolution—that is, switching the occupancy of a single lattice site from "Ag" to "vacancy" and (ii) diffusion—that is, interchanging components (Au and vacancy) on neighboring lattice sites. On a rigid lattice, these are local processes which leave the external dimensions of the body invariant, a statement which holds even if one of the components consists of vacancies.

As a notable exception to the above statement, the external surface will recede by one interplanar spacing every time the outermost lattice plane is removed by

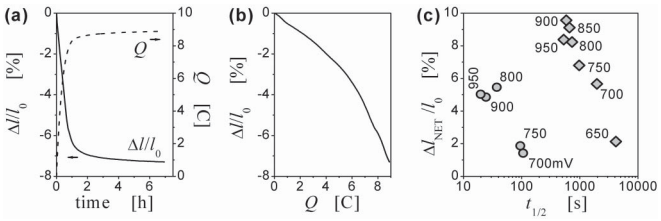

FIG. 3. (a): *In situ* dilatometry traces for bulk (0.9 mm edge-length cubes) $Ag_{75}Au_{25}$ showing the time evolution of relative length change $\Delta l/l_0$ and of transferred charge Q at dealloying potential 850 mV versus Ag/AgCl. (b) $\Delta l/l_0$ versus Q for the data in (a). (c) Net length change after completion of dealloying versus the half-time of dealloying for bulk (◆) and leaf (●; 11 carat) samples. Data points are labeled according to applied potential.

transport of Au atoms from that surface into the interior of the porous layer. In view of the unusually large surface diffusion coefficient of Au at the metal-electrolyte interface (see references in Ref. [10]), this might appear to be the most obvious shrinkage mechanism in the very first stages of dealloying, when the dissolution occurs near the macroscopic sample surface. However, as the dissolution front propagates into the bulk, the diffusion distance to the surface increases, so that the rate of transport should diminish and shrinkage eventually come to a halt for sufficiently deep dealloying. The observation of very similar amounts of shrinkage in leaf and bulk samples, in spite of almost 4 orders of magnitude difference in thickness, as well as the continued shrinkage in the bulk sample even at the very end of the dissolution, when the dealloying front has moved hundreds of microns below the sample surface, argue against this explanation. Furthermore, the large *lateral* shrinkage observed in the Au leaf cannot be explained by the condensation of vacancies at its surface, which would only reduce the thickness.

In addition to the above concerns is the problem of identifying a driving force for long-range transport of matter between the surface and an underlying porous layer. Curvature-driven coarsening is based on transport of matter from positively curved regions on the surface to negatively curved ones. Since the ligaments exhibit saddle-point-like features with highly nonuniform values of the mean curvature, coarsening is expected to proceed predominately by local transport on the scale of the ligament length (order of 10 nm) rather than by long-range transport to the outer surface (up to hundreds of microns). Thus, curvature-driven surface diffusion is likely not the mechanism leading to shrinkage. By a similar argument, grain boundaries can be ruled out as sinks for vacancies: Due to the large grain size, the transport distance is too large.

We shall now speculate on additional processes that could rationalize the experimental finding. As diffusion and elastic distortion can be ruled out (cf. the insignificant change in lattice parameter), it appears that plastic deformation needs to be taken into consideration. While this notion is supported by our observation of an increasing defect density at higher E_D, correlating with the increasing shrinkage, none of the processes below has been confirmed.

The idea of ligament shear touches on an issue of great interest in nanomechanics: In small cylindrical bodies, the surface-induced stress is not hydrostatic [15], and it has been suggested that this may cause spontaneous shear of Au ligaments [16]. Dislocation-mediated shear would require dislocation nucleation, which is an unresolved issue in nanostructures [17], and simulations of tensile loading suggest a transition from dislocation nucleation to homogeneous slip at a ligament diameter of $\sim$1.5 nm [18]. In any case, surface stress-induced compressive yielding is expected to occur only in ligaments with diameters of several nanometers or less [16]. Although this diameter is rather smaller than that observed *ex situ* (Fig. 1), it is conceivable that such small diameter ligaments exist as a transient state, subject to rapid coarsening.

All attempts at rationalizing the shrinkage in terms of dislocations appear to require a mechanism for the formation of dislocations, since a large number of these defects are required to explain the large shrinkage. The injection, at the dissolution front, of lattice vacancies or divacancies [19] into the bulk and their subsequent clustering to form dislocation loops is fraught with controversy [20–23] and should be considered with caution, for, at the very least, it requires that the potential is sufficiently large to enable the dissolution of terrace atoms rather than kink or step atoms, the subsequent burial of the terrace vacancies formed, and the fast motion of the ensuing bulk vacancies. A more plausible process is that sufficiently small pores could collapse to form a planar crystallographic fault bounded by a dislocation loop, reducing their net surface energy in favor of the strain energy of the loop, similar to the collapse of vacancy clusters in bulk crystals [24].

All processes considered above become more likely as the dissolution rate increases since this drives the surface at the dealloying front further away from equilibrium, thereby decreasing the ligament and pore sizes (cf. Fig. 1). This notion agrees with the observation of more shrinkage at faster dissolution in the bulk and leaf samples. It also agrees with the absence of noticeable shrinkage in NPG produced by the slower electronless process of Ref. [11].

It is expected that the processes at the dealloying front depend on the electrode potential not only through the dissolution rate but also through the dependency of formation enthalpy and diffusion constants of surface adatoms and surface vacancies on the electrode potential. The issue is intricately linked to the adsorption of hydroxide at positive electrode potentials. In this respect, it is noteworthy that the shrinkage is indeed reduced at a lesser potential, where hydroxide adsorption is weak. It is also significant that considerable shrinkage is observed throughout the entire potential range studied, indicating that the observation may be relevant for the ''typical'' conditions of dealloying experiments, which will not generally be free of hydroxide adsorption.

In summary, our study shows a quite unexpected dimension change during dealloying of Ag-Au in spite of the retention of the crystal lattice structure in that system. We suggest that plastic deformation, which could arise by homogeneous slip in small ligaments or by climb of lattice dislocations, provides the most obvious mechanism. Thus, as studies of dealloying turn from understanding corrosion towards learning how to make porous nanomaterials for structural or functional applications, materials science issues such as lattice defects and plasticity may emerge as new aspects in the field.

We acknowledge the assistance of Martina Nothacker in preparing some of the samples.

*Electronic address: joerg.weissmueller@int.fzk.de

[1] G. Tammann, Z. Anorg. Allg. Chem. **107**, 1 (1919).
[2] R. C. Newman, S. G. Corcoran, J. Erlebacher, M. J. Aziz, and K. Sieradzki, MRS Bull. **24**, 24 (1999).
[3] M. Raney, Ind. Eng. Chem. **32**, 1199 (1940).
[4] R. W. Ertenberg, B. Andraka, and Y. Takano, Physica (Amsterdam) **284B–288B**, 2022 (2000).
[5] Y. Ding, M. W. Chen, and J. Erlebacher, J. Am. Chem. Soc. **126**, 6876 (2004).
[6] D. Kramer, R. N. Viswanath, and J. Weissmüller, Nano Lett. **4**, 793 (2004).
[7] A. M. Hodge, J. Biener, L. L. Hsiung, Y. M. Wang, A. V. Hamza, and J. H. Satcher, Jr., J. Mater. Res. **20**, 554(2005).
[8] A. J. Forty and P. Durkin, Philos. Mag. A **42**, 295 (1980).
[9] J. Erlebacher, M. J. Aziz, A. Karma, N. Dimitrov, and K. Sieradzki, Nature (London) **410**, 450 (2001).
[10] J. Erlebacher, J. Electrochem. Soc. **151**, C614 (2004).
[11] Y. Ding, Y.-J. Kim, and J. Erlebacher, Adv. Mater. **16**, 1897 (2004).
[12] R. N. Viswanath, D. Kramer, and J. Weissmüller, Langmuir **21**, 4604 (2005).
[13] J. Biener, A. M. Hodge, and A. V. Hamza, Appl. Phys. Lett. **87**, 121908 (2005).
[14] B. G. Ateya, G. Geh, A. H. Carim, and H. W. Pickering, J. Electrochem. Soc. **149**, B27 (2002).
[15] J. Weissmüller and J. W. Cahn, Acta Mater. **45**, 1899 (1997).
[16] J. Diao, K. Gall, and M. L. Dunn, Phys. Rev. B **70**, 075413 (2004).
[17] J. Weissmüller and J. Markmann, Adv. Eng. Mater. **7**, 202 (2005).
[18] M. R. Sørensen, M. Brandbyge, and K. W. Jacobsen, Phys. Rev. B **57**, 3283 (1998).
[19] H. W. Pickering and C. Wagner, J. Electrochem. Soc. **114**, 698 (1967).
[20] A. V. Vvedenskii and I. K. Marshakov, Russ. J. Electrochem. **31**, 234 (1995).
[21] J.-Y. Zou, D.-H. Wang, and W.-C. Qiu, Electrochim. Acta **42**, 1733 (1997).
[22] Yu. Ya. Andreev and A. V. Goncharov, Electrochim. Acta **50**, 2629 (2005).
[23] E. Schofield, Trans. Inst. Met. Finish. **83**, 35 (2005).
[24] T. L. Davis, J. Appl. Phys. **38**, 3756 (1967).